2G/3G Serpentine Shape Inverted-F Antenna for Near Body Application

Mehdi Seyyedesfahlan[1], Nuno Pires[2] and Anja K. Skrivervik[1]
[1]*Microwave and Antenna Group, Ecole Polytechnique Fédérale de Lausanne, CH-1015 Lausanne, Switzerland*
{mehdi.esfahlan, anja.skrivervik}@epfl.ch
[2]*Geosatis SA, Rue Saint-Hubert 7, CH-2340 Le Noirmont, Switzerland*
nuno.pires@geo-satis.com

***Abstract*—In this contribution, we present a miniature antenna placed in a leg bracelet for body worn applications. It operates in both the 820-960 MHz and the 1.7-2.1 GHz bands. The radiating element, based on an inverted-F antenna, occupies a 37 mm × 37 mm area and is printed on a flexible substrate that extends a multilayer circuit board. The serpentine shape helps to widen the bandwidths as well as minimize the size. The antenna is characterized for different situations: standalone, inside the plastic casing and worn close to the body inside the same casing. Both simulations and measured results are presented, and they agree well. The design steps are reviewed with the aid of current distribution simulation plots.**

***Index Terms*—small antenna, antenna for 2G/3G application, body impact on antenna S_{11}.**

I. Introduction

In recent years, the demand for tracking devices able to communicate using mainstream technologies is increasing. Typical applications can be found in vehicles or used near the body resorting to Bluetooth, 2G/3G, GPS and LTE. Designing multi-band antennas for such systems, can be a challenge when the available volume is limited, as they must be robust to the deployment environment, even more so close to the body applications [1]. Relevant examples are the small patch antenna developed in [2] to cover GSM 850, 900 and 1800 MHz bands; a loop antenna incorporated with a monopole to be used in a tablet computer considering on-body specific absorption ratio (SAR) in [3]; the small-size complicated monopole antenna designed in [4] and the body distance influence on antenna performance study of [5].

In this paper, we present an antenna, designed for the 2G/3G bands to be integrated with the controlling electronic circuit inside an ankle bracelet. The antenna is tested in different situations, such as in free space, inside the casing and when the bracelet is worn on the leg. Additionally, the impact of the ground, the casing and the body on antenna performances is studied by modelling and simulating the antenna in these different situations. Then, the precision of the models and real body impact is confirmed by multiple measurements. The paper is organized as follows: in section II, the antenna structure is introduced, followed by the description of the simplified simulation models for antenna and casing and body phantom in III. Section IV shows and discusses the antenna measurement and simulation results followed by the conclusion in section V.

This work was supported in part by the Swiss Commission for Technology and Innovation (CTI) under Grant 25752.2 PFNM-NM.

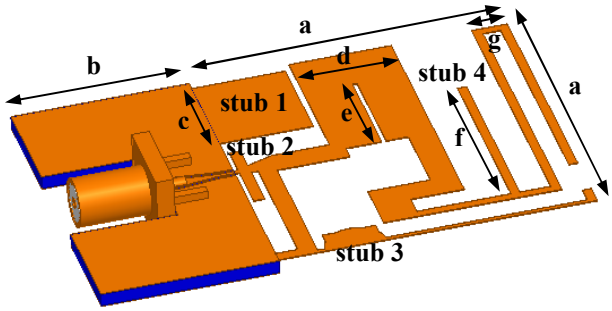

Fig. 1. Optimized antenna configuration. Antenna dimensions (in mm) are a = 37, b = 20, c = 11.5, d = 11.5, e = 12, f = 22, and g = 4.

II. Antenna Design in Free Space

The considered antenna is displayed in Fig. 1. The feeding point, which is placed in the centre of the edge of the ground plane, is a 50 Ω grounded back coplanar waveguide (GBCPW) transmission line. The ground plane and transmission line are built in FR4 substrate (ε_r = 4.1, h = 1.6mm) while the radiating element is made of a thick sheet of copper in air. The antenna is intended to work in dual band, namely, 820-960 MHz and 1.7-2.1 GHz. The structure is an inverted-F antenna, which is tuned in the two bands using four stubs at different positions. The stubs couple with different parts of antenna and enhance the antenna matching by adding resonances into the desired bands.

The antenna input reflection coefficient magnitude (S_{11}) and the influence on the same parameter of the slot (the length with letter *e* in Fig. 1) and four stubs are presented in Fig. 2. The proposed antenna S_{11} is below -6 dB between 878-1013 MHz and 1.52-2.26 GHz. The lower frequency interval is slightly above the desired band of 820-960 MHz but, at the initial design phase, the dielectric casing effects were not considered and are expected to lower the antenna operating frequency, as confirmed in IV.

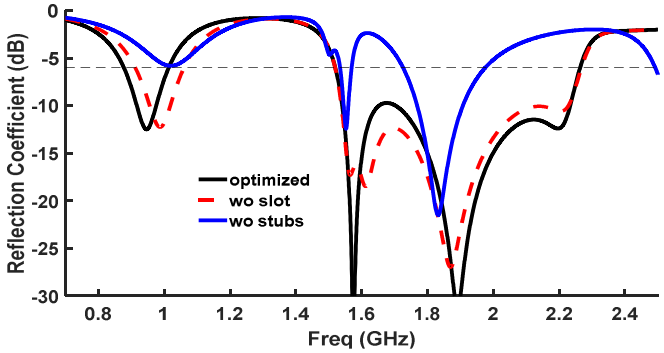

Fig. 2. Reflection coefficient of optimized antenna and the effects of the removal of slot (red) and stubs (blue).

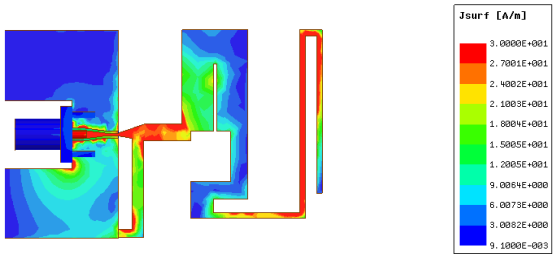

Fig. 3. Current distribution on the antenna without stubs at f = 1830 MHz.

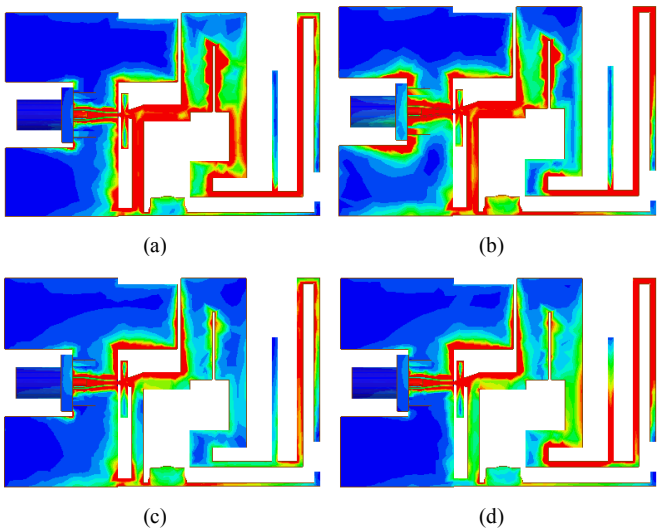

Fig. 4. Current distribution on the proposed antenna at (a) 947 MHz, (b) 1570 MHz, (c) 1890 MHz and (d) 2200 MHz.

When the slot is removed (red curve in Fig. 2) the current path at the lower frequencies becomes shorter. Hence, a 41 MHz up-shift is observed in the lower band resonance.

When all four stubs are removed, as shown in Fig. 3 for the frequency having the lower S_{11} (1830 MHz), the blue curve of Fig. 2 keeps its overall shape compared with the original antenna (in black), but with an important degradation of the matching.

The current distribution on the antenna with slot and stubs is shown in Fig. 4 at four different resonant frequencies. The current distributions at the same frequencies are shown in Fig. 5 when the stubs are absent from the structure. Fig. 6 compares the S_{11} of the optimised, structure to the same

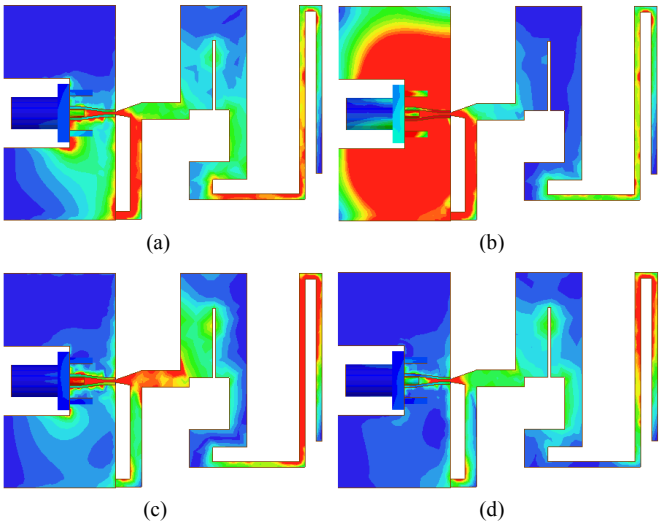

Fig. 5. Current distribution on the antenna with removed stubs at (a) 947 MHz, (b) 1570 MHz, (c) 1890 MHz and (d) 2200 MHz.

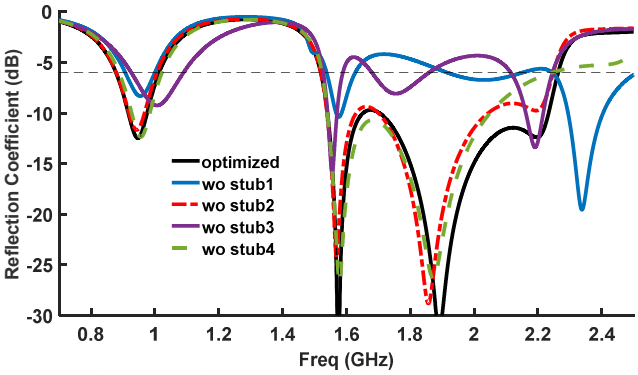

Fig. 6. Reflection coefficient of optimized antenna and influence of each stub on the magnitude of antenna *S11*.

parameter when only a single stub is removed, demonstrating how each contributes to tune the antenna in different frequencies at both relevant bands.

By comparing Figs. 4 and 5, and looking at Fig. 6, it is apparent that *stub1* plays a very important role in the upper band, in improving the antenna matching by adding different paths to the current. *Stub2*, which is placed near the feeding point and parallel to ground plane, couples directly to the edge of the ground and adds a local capacitance. This enhances the current flow toward the radiating element from the feeding line, and results in an upper band widening, as confirmed in Fig. 6. Both *stub1* and *stub2* enhance the matching of the antenna at all considered frequencies, by adding a capacitance between antenna and ground. *Stub 3* results in an improved match in the higher band and indeed, comparing Figs. 4(c) and 5(c) demonstrates the current flow from the feed to the main arm of the antenna, an area where the current distribution is very low in absence of this stub. Moreover, it lowers the lower frequency band. The influence of *stub4* is apparent in Fig. 4(d), expanding the upper band by providing an additional resonance at 2.2 GHz.

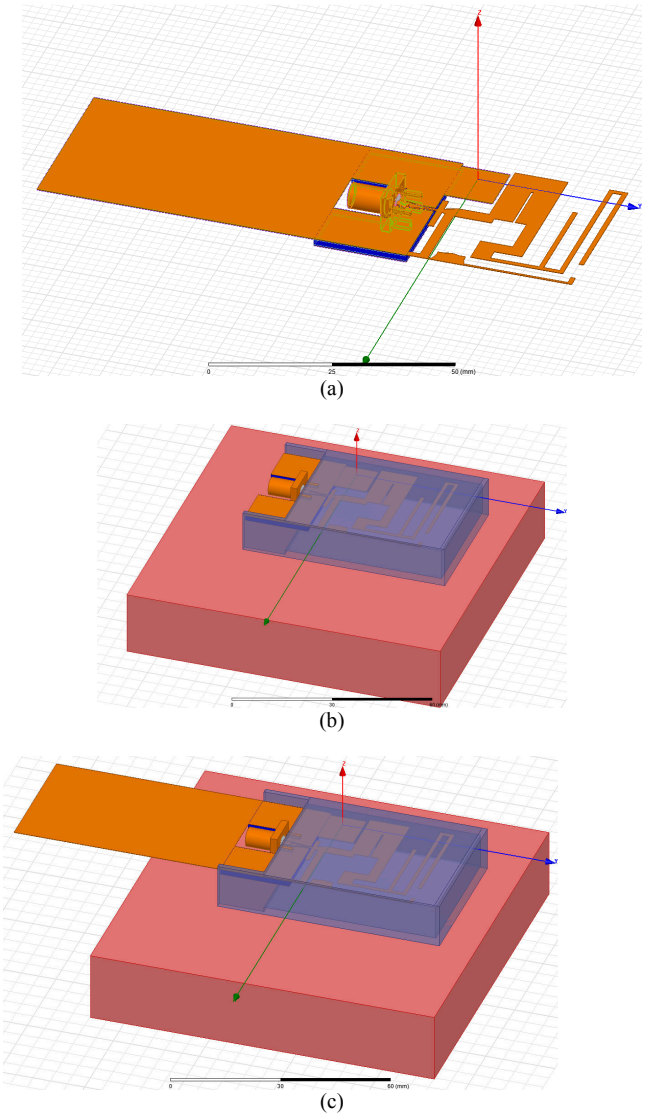

Fig. 7. Different models used for the antenna simulations: (a) antenna in free space, (b) antenna with body phantom (pink block) and casing (blue block), and (c) antenna with body phantom and casing and large ground plane.

III. Casing and Body Model

As mentioned in Section I, the aim of the presented antenna is to be used inside a dielectric casing worn on the leg. In the design phase, the device casing and the body were modelled by parallelepiped blocks of material in order to keep the calculation time low. The simulations therefore only consider the portions of casing and limb which are near the antenna. This choice stems from the fact that the antenna has small details requiring fine meshes and these become very computationally expensive when simulated close large volumes of dielectric material.

Fig. 7(a) shows the antenna of Fig. 1 with the ground extended by 60 mm using a copper strip in order to consider the effect of the PCB connected to the antenna. Figs. 7(b) and (c) show the antenna without and with this extended ground plane, respectively, surrounded by the casing (blue) close to the body (pink). The casing is modelled using dielectric walls with thicknesses of 1.5 mm and a dielectric permittivity of 3, while a block with dimensions 100×100×20 mm^3 is used for the muscle model with properties given in [6] for the different frequency bands.

IV. Simulation and Measurement Results

The antenna was built and tested in different situations to verify the accuracy of the simulation models and results.

The fabricated antenna in free space and inside the real casing worn on the leg are shown in Fig. 8. We notice that the radiating element is flexible and can easily be placed inside the toroidal ankle bracelet and fed using a coaxial bend and cable.

Four experiments were done to characterize the antenna reflection coefficient: 1) proposed antenna in free space, 2) proposed antenna on the leg, 3) extended ground in free space and 4) extended ground worn on the leg.

Fig. 9 shows the simulated and measured antenna reflection coefficient in free space. The results agree in the lower band, but there is a slight frequency shift between simulation and measurement in the higher band. This can be explained by the low fabrication precision of stubs 2 and 4 that were confirmed in simulation to be important for higher frequency performance in the presented curves in Fig. 6. The same cause can be attributed to the double resonance at the lower edge of the upper band in the measured results: in the measurement, due to slight change in the shape and dimensions of stub2, a small inductance is added to the mostly capacitive effect of this stub.

The influence of the casing, the body and the long ground plane are presented in Fig. 10(a) and (b) for simulations and measurements in realistic conditions, respectively. Increasing the length of ground plane will affect the lower band and shift it to lower frequencies, and enhance the antenna matching in the lower band. As it is expected, the presence of the body will shift the antenna's S_{11} to lower frequencies. Using the antenna near the body will also reduce the bandwidth in both bands. Figs. 10(a) and (b) show that the simple casing and body models used in the simulations are adequate for the upper band and show results similar to the measurements. However, and as expected due to the larger wavelength, the results diverge more

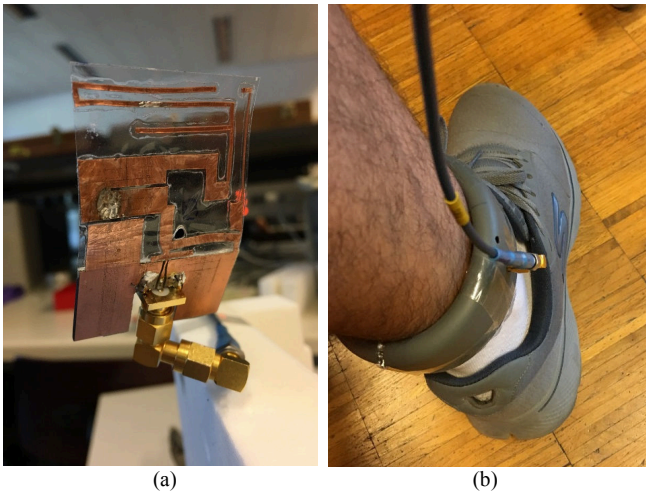

Fig. 8. Fabricated antenna (a) alone in the free space, (b) worn on the leg.

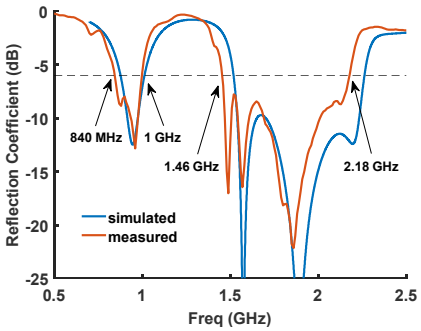

Fig. 9. Antenna simulated and measured reflection coefficient as is placed alone in free space.

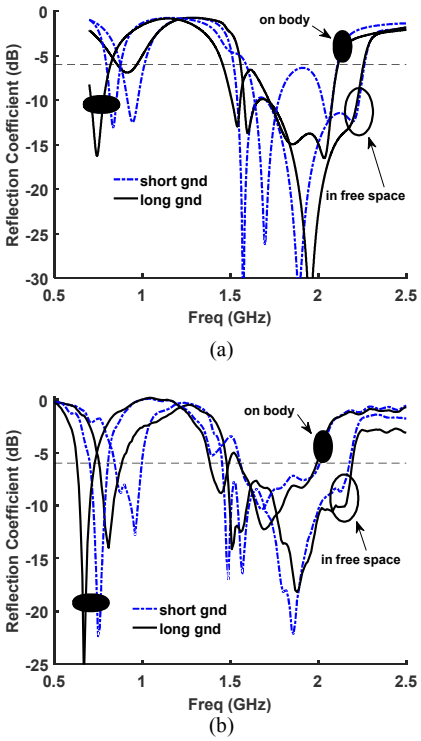

Fig. 10. Antenna (a) simulated and (b) measured reflection coefficient as its ground is short (dash-dot), long (solid), in free space, worn on the leg (full ellipse).

in the lower band. This can be addressed by increasing the dimensions of the simulation box but would make the simulation time prohibitively large in an interactive antenna design process.

V. Conclusions

An inverted-F antenna that includes four tuning stubs was presented. The antenna and ankle bracelet on body were modelled and characterized for the input reflection coefficient. The measurement and simulation for the antenna in free space agree well, confirming the accuracy of the antenna simulation model. The validity of the simplified casing and ankle models was demonstrated for the upper band and, despite the lower accuracy in the lower band, it is still useable for interactive design purposes. The electronic circuit board feeding the antenna was modelled by increasing the length of ground plane. The measured and simulation results for the worn bracelet, on the leg, showed that the antenna *S11* curve keeps its shape for both cases; however, an 80 MHz shift for the lower band is observed.

References

[1] A. Nella, and A. S. Gandhi, "A survey on microstrip antennas for portable wireless communication system applications," *International Conference on Advances in Computing, Communications and Informatics (ICACCI)*, 2017, pp. 2156-2165.

[2] N. H. Nguyen, K. T. Liem, N. D. Uyen, and D. P. Duy, "A Small Patch Antenna for GSM Applications," *IEEE Fifth International Conference on Communications and Electronics (ICCE)*, 2014, pp. 395-398.

[3] K.-L. Wong, W.-J. Wei, and L.-C. Chou, "WWAN/LTE Printed Loop Tablet Computer Antenna and Its Body SAR Analysis," *Microwave and Optical Technology Lett.*, vol. 53, no. 12, pp. 2912-2919, Sep. 2011.

[4] J.-H. Lu, and Y.-S. Wang, "Planar Small-Size Eight-Band LTE/WWAN Monopole Antenna for Tablet Computers," *IEEE Trans. Antennas Propag.*, vol. 62, no. 8, pp. 4372-4377, Jun. 2014.

[5] T. Tuovinen, T. Kumpuniemi, K. Y. Yazdandoost, M. Hämäläinen, and J. Iinatti, "Effect of the Antenna-Human Body Distance on the Antenna Matching in UWB WBAN Applications," *7th International Symposium on Medical Information and Communication Technology (ISMICT)*, 2013, pp. 193-197.

[6] https://itis.swiss/virtual-population/tissue-properties/database/dielectric-properties/